

ARTICLE

ERp29 Is a Ubiquitous Resident of the Endoplasmic Reticulum with a Distinct Role in Secretory Protein Production

Steven D. Shnyder¹ and Michael J. Hubbard

Department of Biochemistry, University of Otago, Dunedin, New Zealand

SUMMARY ERp29 was recently characterized biochemically as a novel protein that resides in mammalian endoplasmic reticulum (ER). Here we applied immunochemical procedures at the cellular level to investigate the hypothesized role of ERp29 in secretory protein production. ERp29 was localized exclusively to the ER/nuclear envelope of MDCK cells using confocal immunocytochemistry and comparative markers of the ER lumen, ER/Golgi membrane, nuclei, and mitochondria. A predominant association with rough ER was revealed by sucrose-gradient analysis of rat liver microsomes. Immunohistochemistry showed ERp29 expression in 35 functionally distinct cell types of rat, establishing ERp29 as a general ER marker. The ERp29 expression profile largely paralleled that of protein disulfide isomerase (PDI), the closest relative of ERp29, consistent with a role in secretory protein production. However strikingly different ERp29/PDI ratios were observed in various cell types, suggesting independent regulation and functional roles. Together, these findings associate ERp29 primarily with the early stages of secretory protein production and implicate ERp29 in a distinct functional role that is utilized in most cells. Our identification of several ERp29-enriched cell types suggests a potential selectivity of ERp29 for non-collagenous substrates and provides a physiological foundation for future investigations.

(*J Histochem Cytochem* 50:557–566, 2002)

KEY WORDS

ERp29
reticuloplasmin
chaperone
protein folding
protein disulfide isomerase
BiP

THE ENDOPLASMIC RETICULUM (ER) is a multifunctional organelle whose principal roles include production of proteins that traverse the secretory pathway, the mobilizable storage of calcium, and lipid metabolism (Gething and Sambrook 1992; Pozzan et al. 1994; Satoh and Hosokawa 1998). The ER contains complex machinery for the production of secretory proteins (Ellgaard et al. 1999). In the ER lumen, soluble resident proteins (reticuloplasmins) participate in the early protein processing events that follow import of nascent polypeptides from ribosomal sites of synthesis (i.e., folding, initial glycosylation, and assembly of oligomers). Several reticuloplasmins are expressed ubiquitously in higher animals, the most common of which are protein disulfide isomerase (PDI) and its relatives

ERp60 and ERp72 (Ferrari and Soling 1999), BiP (Gething 1999), calreticulin (Michalak et al. 1999), and endoplasmin (Argon and Simen 1999). These major reticuloplasmins constitute >1% of soluble protein in protein secretory cells and serve a variety of general and overlapping roles. First, all function as molecular chaperones that shield hydrophobic sequences and thereby foster the proper folding of nascent proteins. Second, all except ERp60 are calcium-binding proteins consistent with the dependence of protein folding on regulated ER calcium levels (Corbett and Michalak 2000). Third, PDI-family members act as “foldases” that catalyze disulfide bond formation. Included in a large group of less common reticuloplasmins are the enzymes that initiate glycosylation of secretory proteins (Parodi 2000) and the ER carboxylesterases involved in lipid metabolism (Satoh and Hosokawa 1998).

ERp29 is a recently discovered ER resident that has been implicated in secretory protein synthesis and appears to be of similar prevalence to the established major reticuloplasmins (Demmer et al. 1997; Hubbard et al. 2000). ERp29 is encoded by a single gene

Correspondence to: Dr. Mike Hubbard, Dept. of Biochemistry, University of Otago, PO Box 56, Dunedin, New Zealand. E-mail: mike.hubbard@stonebow.otago.ac.nz

Received for publication September 4, 2001; accepted November 28, 2001 (1A5629).

¹Present address: Cancer Research Unit, University of Bradford, Bradford, UK.

in humans that has been highly conserved during mammalian evolution (Hubbard and McHugh 2000). The novel protein sequence of ERp29 exhibits characteristic features of a reticuloplasm (signal peptide, ER retention motif), and localization to the ER lumen was comprehensively supported at the biochemical level (Demmer et al. 1997; Ferrari et al. 1998; Mkrtchian et al. 1998b; Hubbard et al. 2000). At 25.6 kD (29 kD on SDS-PAGE), ERp29 is considerably smaller than the major reticuloplasm (46–95 kD) and comprises only two principal folding domains (Demmer et al. 1997; Liepinsh et al. 2001). The N-terminal domain is homologous to thioredoxin-like domains in PDI, but ERp29 lacks the redox-active Cys-X-X-Cys motifs common to all PDI family members. Other distinctive properties of ERp29 are an absence of calcium-binding motifs and the lack of classical (BiP-like) stress responsiveness (Demmer et al. 1997; Ferrari et al. 1998). Using immunoblotting analysis, we found ERp29 to be broadly distributed and particularly abundant in protein secretory tissues. Moreover, the molar ratios of ERp29, PDI, and BiP varied among tissues, suggesting a link between the type of secretory product and ERp29 abundance (Hubbard et al. 2000). Together, these biochemical findings identified ERp29 as a new class of reticuloplasm that potentially has a novel and major role during secretory protein production.

Despite good progress with biochemical understanding, no functional activity has been established for ERp29 to date (Liepinsh et al. 2001). Little has been learned about ERp29 at the cellular level and therefore a variety of functionally informative avenues remain to be explored. We have now used immunoblotting procedures to characterize the subcellular location and cellular distribution of ERp29 in detail, aiming to address the hypothesis that ERp29 participates in early phases of secretory protein synthesis. It was not clear from preliminary immunolocalization data (Ferrari et al. 1998; Mkrtchian et al. 1998b) if ERp29 is present in distal compartments of the secretory pathway where addition of terminal carbohydrates and lipids occurs (Parodi 2000) or in mitochondria and nuclei, as suggested by subcellular fractionation of liver (Hubbard et al. 2000). Several reticuloplasm are not restricted to the ER (Takemoto et al. 1992; Ellgaard et al. 1999; Michalak et al. 1999; Honore and Vorum 2000; Holaska et al. 2001), including calreticulin, which was used as reference for ERp29 immunolocalization (Ferrari et al. 1998). Consequently, we used confocal microscopy with a variety of comparative markers to localize ERp29 in a secretory cell line. It was also unknown whether the broad tissue expression of ERp29 reflected a ubiquitous cellular distribution or one restricted to a variety of broadly distributed cells. To evaluate this question and the postulated link with type of secretory product

(Hubbard et al. 2000), we have done an extensive immunohistochemical analysis comparing the expression of ERp29 with that of its closest structural relative, PDI.

Our results suggest that ERp29 is primarily involved in early protein processing events and that its role is significant in most cell types and selective for particular types of secretory protein. We have also identified a variety of cells in which ERp29 is likely to have particular functional importance and in which candidate protein substrates of ERp29 can be pursued.

Materials and Methods

Proteins and Antibodies

Rat liver ERp29 and rabbit antiserum to this protein were prepared as outlined elsewhere (Hubbard and McHugh 2000). Polyclonal antibodies to ERp29 (anti-ERp29) were subsequently isolated by microscale affinity purification (Hubbard 1995) using rat ERp29 conjugated to CNBr-Sepharose (from Amersham Pharmacia Biotech; Auckland, NZ) as ligand, and characterized by immunoblotting. PDI and calreticulin were purified to homogeneity (assessed by SDS-PAGE and N-terminal sequencing) from side fractions of the ERp29 preparations, using non-denaturing column chromatographies over DEAE-Sepharose, heparin-Sepharose, Resource-Q (from Amersham Pharmacia Biotech), and hydroxyapatite (from BioRad; Hercules, CA). Antisera to PDI and calreticulin were raised conventionally in New Zealand White rabbits (Hubbard 1995), and anti-calreticulin was prepared by affinity purification and characterized as outlined for anti-ERp29. The PDI antiserum exhibited high avidity (i.e., effective at $>10^4$ -fold and 10^3 -fold dilutions for immunoblotting and immunolocalization, respectively) and so was used without purification (anti-PDI). Antibodies to BiP and endoplasm (goat polyclonals to peptide immunogens) were from Santa Cruz Biotechnology (Santa Cruz, CA), and the anti-mitochondrial cytochrome c oxidase (mouse monoclonal) was from Molecular Probes (Eugene, OR). Monospecificity of the commercial antibodies was verified by immunoblotting.

Cell Culture

MDCK cells (ATCC CCL-34), derivatives of canine renal tubule epithelium (Meier et al. 1983), were kindly provided by Dr J. Bedford (Physiology Department, Otago University). Cells were cultured conventionally in low-glucose DMEM containing 10% fetal bovine serum and antibiotic/antimycotics (all products of Invitrogen; Auckland, NZ), and passaged biweekly. Just before experiments, growth medium was removed and the cells washed twice in Tris-saline (10 mM Tris-HCl, pH 7.2, at 20°C, 160 mM NaCl) either at room temperature (RT) or on ice (before fixation and protein extraction, respectively).

Rat Tissues and Extracts

All animal procedures were undertaken in accordance with the ethical requirements of this institution. Wistar-derived rats were given unlimited access to a standard pellet chow and maintained conventionally (Hubbard 1995). Dental tis-

sues (hemimandibles) were excised rapidly from decapitated neonates (5–15 days old). Other tissues were taken from juveniles (8–10 weeks old) immediately after asphyxiation with CO₂ and decapitation. Isolated tissues were washed twice in Tris-saline before fixation or storage (–80C).

Triton-soluble proteins were extracted from MDCK cells and rat tissues by mechanical dispersion in 4 tissue-vol. of ice-cold Triton homogenization buffer (0.5% Triton X-100 in 10 mM Tris-HCl, pH 7.2, 10 mM EGTA, 5 mM dithiothreitol, 1 mM aminoethylbenzene sulfonyl fluoride, 1 mM benzamidine, 5 µg/ml leupeptin, 5 µg/ml pepstatin), followed by centrifugation for 5 min at 20,000 × g (Hubbard and McHugh 2000). Rat liver microsomes were prepared as before (Demmer et al. 1997; Hubbard et al. 2000) except, in the subfractionation experiments (Figure 3), source animals were fasted for 20 hr before tissue isolation.

Immunolocalization in Cells and Tissues

All immunolabeling incubations were done at RT in a dark humidified chamber, and all intermediate washes involved three exposures to Tris-saline (each 2–5 min at RT). Fixatives were prepared in Sorenson's PBS, and antibodies and fluorescently-labeled probes were diluted in Tris-saline, unless indicated otherwise. Antibody solutions additionally contained normal serum (Vector Laboratories; Burlingame, CA) from a species appropriate to each antibody (i.e., goat, rabbit, and horse sera were used with antibodies from rabbit, goat, and mouse, respectively). Specificity of immunolabeling was assessed in control experiments in which primary antibody was omitted or replaced with an equivalent concentration of non-immune IgG, as illustrated for immunoblotting (Figure 1).

For immunocytochemistry, MDCK cells grown for 24 hr on uncoated glass coverslips were fixed for 30 min in 4% paraformaldehyde (EM grade, from ProSciTech; Thuringowa, Australia), washed, and then quenched with antibody diluent (Tris-saline containing 0.1% Triton and 3% normal serum) for 15 min. For green channel immunolabeling (488 nm), cells were exposed to anti-ERp29 (4 hr), washed, then incubated in Oregon Green-labeled secondary antibodies (goat anti-rabbit; from Molecular Probes) for 30 min. After washing, the cells were again quenched in antibody diluent for 10 min. For red channel labeling (568 nm), anti-ERp29-labeled cells were either (a) incubated in anti-BiP or anti-cytochrome c oxidase (2 hr), washed, and then exposed to biotinylated secondary antibody (rabbit anti-goat or horse anti-mouse, respectively; from Vector Laboratories) for 30 min. After washing, the cells were incubated with Cy3-labeled streptavidin (from Amersham Pharmacia Biotech) for 30 min; (b) digested with RNase (100 µg/ml in Tris-saline, from Roche; Auckland NZ) for 10 min, then incubated for 5 min in propidium iodide (1 µg/ml in deionized water; from Molecular Probes); (c) incubated for 20 min in Texas Red-labeled concanavalin A (200 µg/ml in 100 mM NaHCO₃, 1 mM MnCl₂, 1 mM CaCl₂; from Molecular Probes). Double-labeled specimens were subsequently washed and mounted under glass coverslips with DABCO/PVA antifade medium (3% 1,4-diazabicyclo(2,2,2)octane, 33% glycerol, 15% polyvinyl alcohol, 67 mM Tris-HCl, pH 8.5; products of Sigma, St Louis, MO). Green and red channel images

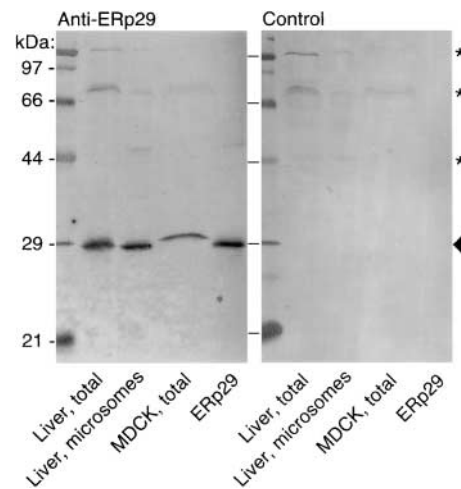


Figure 1 Monospecific immunodetection of ERp29 in liver and MDCK cell extracts. Triton-soluble proteins from whole rat liver, rat liver microsomes, and confluent MDCK cells were immunoblotted with affinity-purified ERp29 antibodies (anti-ERp29) and non-immune IgG (Control) as indicated. The 29-kD ERp29 band was predominant and detected specifically (arrowhead). Minor bands at 120-, 80-, and 48 kD were detected nonspecifically (asterisks) and corresponded to naturally biotinylated proteins identified earlier (Hubbard 1995). The slower migration of canine ERp29 probably reflects the fivefold higher protein load needed to equate immunoreactivity with the rat tissue samples. We previously reported that the electrophoretic mobility of ERp29 is sensitive to protein load variations (Hubbard and McHugh 2000).

were obtained separately with a confocal laser scanning microscope (BioRad MRC600) and processed using publically available software (Image, from NIH, Bethesda, MD; Photoshop, from Adobe Systems, Mountain View, CA; and Canvas, from Deneba, Miami, FL).

For immunohistochemistry (Table 1, Figure 4), freshly isolated tissues were fixed by immersion in 10% neutral-buffered formalin and slowly mixed for 24 hr. Immunostaining of dental tissues was found to be more homogeneous (e.g., Figure 4A) in samples prefixed by transcardial perfusion (PBS followed by 4% paraformaldehyde at 80–100 mm Hg for 5 min). Mineralized tissues were decalcified by overnight incubation in chelator (7.5% neutralized EDTA in 10% neutral-buffered formalin) followed by three microwave treatments (15 sec at medium power, each with fresh chelator). Paraffin sections (6 µm thick on coated slides, prepared conventionally by the Otago University Histology Service Unit) were dewaxed (xylene, then 100% ethanol), treated with peroxide to block endogenous peroxidase activity (freshly prepared 0.15% H₂O₂ in 100% methanol for 30 min) and then rehydrated through an ethanol series. After quenching in antibody diluent for 20 min, sections were exposed to primary antibodies (diluted in normal serum) for 16 hr, washed, incubated with biotinylated secondary antibody (goat anti-rabbit) for 60 min, and washed again. For color development, sections were incubated with the Vectastain ABC-peroxidase (30 min) and diaminobenzidine substrate reagents (Vector Laboratories), then stopped with water washes. After nuclear counterstaining with Gurr's hematoxylin (from BDH; Palmerston North, NZ), the

Table 1 Comparative immunohistochemical analysis of ERp29 and PDI expression in rat

Tissue type or organ	Cell type	Immunostaining ^a	
		ERp29	PDI
Adrenal gland	Cortical cells	++	++
	Medullary cells	++	++
Bone (femur)	Osteoblasts	++	++
	Chondrocytes, epiphyseal	+	++
	Marrow	++	++
Brain	Purkinje cells, cerebellum	+++	+
	Granule cells, cerebellum	+	++
	CA1 neurons, hippocampus	++	++
Gastrointestinal tract	Stomach epithelium	++	++
	Duodenal epithelium	++	+ / ++
	Duodenal lymphocytes	++	+ / ++
	Colon epithelium	++	++
Integument	Colon lymphocytes, Peyer's	++	+ / ++
	Epidermis	++	+++
	Dermal fibroblasts	+ / ++	+++
	Hair follicle	++	++
Kidney	Sebaceous acini	+	+
	Glomerulus	+	+
	Tubules	++	++
Liver	Capsule adipocytes	+	+
	Hepatocytes	+ / ++	++
Lung	Endothelial cells	+	+
	Type 1 alveolar cells	+	+
	Type 2 alveolar cells	+++	+++
Mammary (lactating)	Clara cells, bronchiole	+	++
	Alveolar epithelium	+++	+++
Muscle	Skeletal striated fibers	nd ^b	nd
	Cardiac myocytes	nd	nd
	Vascular smooth myocytes	+	nd
Ovary	Follicle cells	++	++
Pancreas	Endocrine islets	++	+
	Exocrine acini	+	++
Salivary (parotid)	Mucous acini	++	++
	Serous acini	+	++
Spleen	White cell precursors	+++	+
	Red cell precursors	+	+
Testis	Spermatogenic epithelium	++	++
Tooth	Ameloblasts	+++	+++
	Odontoblasts	+	++
	Pulp, fibroblasts	+	++
Uterus	Endometrium	++	++

^a+, weak; ++, moderate; +++, strong.

^bNot detected substantially above background levels of non-immune controls and erythrocytes (no ER).

sections were dehydrated, cleared in xylene, and mounted (DPX mountant, from BDH) conventionally. Micrographs were recorded on color transparency film (Agfa Optima, 100 ASA) with a Leitz Orthoplan microscope, then scanned and processed digitally as above.

Other Procedures and Materials

Rat liver microsomes were subfractionated by centrifugation (160,000 × g, 19 hr) on discontinuous sucrose density gradients as described (Kreibich et al. 1978; Hortsch and Meyer 1985). The separation efficacy was confirmed by UV spectrometry and SDS-PAGE (not shown). SDS-PAGE with Co-

massic staining, and immunoblotting analyses were done with established procedures (Hubbard 1995; Hubbard et al. 2000). Immunoblots were developed using avidin/biotin amplification (Vectastain ABC-peroxidase and diaminobenzidine), and antibody dilutions were optimized so that individual immunoblots could be probed with multiple antibodies in parallel. Imaging densitometry was done under linear conditions established with varied sample loads.

Results

Preparation of Monospecific Antibodies to ERp29

To undertake cellular localization of ERp29, we prepared polyclonal antibodies to ERp29 purified from rat liver. Anti-ERp29 immunoblot analysis (Figure 1) showed that ERp29 was recognized with high specificity in a complex protein extract from Triton-solubilized rat liver. Moreover, no crossreaction with other ER proteins was evident in an enriched extract from rat liver microsomes. Canine ERp29 was also recognized specifically in the Triton-soluble extract from a dog kidney cell line (MDCK) although fivefold higher protein loadings were required compared with rat liver. The reduced immunoreactivity towards canine ERp29 could reflect a cross-species bias because these antibodies exhibited a 30-fold lower avidity for human ERp29 than for the rat orthologue used as immunogen (Hubbard and McHugh 2000). We concluded that the anti-ERp29 was monospecific and suitable for immunolocalization studies in rat tissues and MDCK cells.

Immunolocalization of ERp29 to ER Exclusively

MDCK cells were selected for investigating the subcellular distribution of ERp29 because the ER and Golgi apparatus are displayed prominently and a variety of proteins are constitutively exported to the plasma membrane and culture medium (Urban et al. 1987). We anticipated that ERp29 would be readily detected in this renal epithelium cell line, given the relatively high expression levels in rat kidney (Hubbard et al. 2000). Difficulty with immunodetection of ERp29 was previously encountered in several other cell lines (Ferrari et al. 1998; Mkrtchian et al. 1998b). To provide a more stringent analysis than before, we localized ERp29 in comparison to a variety of established markers using dual-label confocal fluorescence microscopy. Finally, our strategy aimed to account for the finding that, after conventional subcellular fractionation of homogenized rat liver, substantial amounts of ERp29 partitioned to the nuclear, mitochondrial, and cytosolic fractions in addition to the expected localization with microsomes (Hubbard et al. 2000).

First, we found that anti-ERp29 revealed a characteristic reticular pattern that was essentially indistinguishable from that of BiP, an archetypal resident of

the ER lumen (Figure 2A). Notably, the immunostaining was most dense in the perinuclear region and decreased towards the cell periphery. ERp29 was also found to co-localize precisely with calreticulin, PDI, and endoplasmic reticulum chaperone (not shown), strengthening previous findings (Ferrari et al. 1998; Mkrtchian et al. 1998b). Second, when propidium iodide was used to reveal nuclei, an exact correspondence was obtained with the perinuclear boundary of ERp29 staining, which was clearly demarcated in favorable optical sections (Figure 2B). This localization to the nuclear envelope is consistent with other reticuloplasmic proteins (Bole et al. 1989) and accounts for the previous finding of ERp29 in crude nuclear fractions (Hubbard et al. 2000). Third, the immunostaining of mitochondrial cytochrome c oxidase exhibited a markedly different pattern from that of ERp29 (i.e., rods vs reticular) and extended to peripheral regions of cytoplasm where ERp29 was lacking (Figure 2C). Fourth, concanavalin A, which labels the ER from nuclear envelope to proximal elements of the Golgi complex (Wood et al. 1974; Bergmann and Fusco 1990), was found to have the same topographical distribution as ERp29 (Figure 2D). No

Golgi-like labeling (i.e., ERp29-positive, concanavalin A-free) was observed. Finally, when the cell perimeter was imaged using autofluorescence, we found no evidence that ERp29 is associated with the plasma membrane (not shown). Together, these results indicate that ERp29 is exclusively located in the ER/nuclear envelope of MDCK cells.

Dominant Association with Rough ER

To address the hypothesis that ERp29 has a role in the early phase of secretory protein synthesis, we next investigated the possibility of a preferential association with rough ER. Although luminal continuity exists between rough and smooth ER, protein-centric BiP was found to predominate in rough microsomes, whereas reticuloplasmic proteins involved in calcium storage and lipid metabolism partitioned more strongly to smooth microsomes (Mentlein et al. 1988; Bole et al. 1989; Villa et al. 1992,1993; Nori et al. 1993). Previously ERp29 was separated from Golgi-enriched fractions on density gradients, but the distribution of ERp29 between rough and smooth ER was not reported (Ferrari et al. 1998).

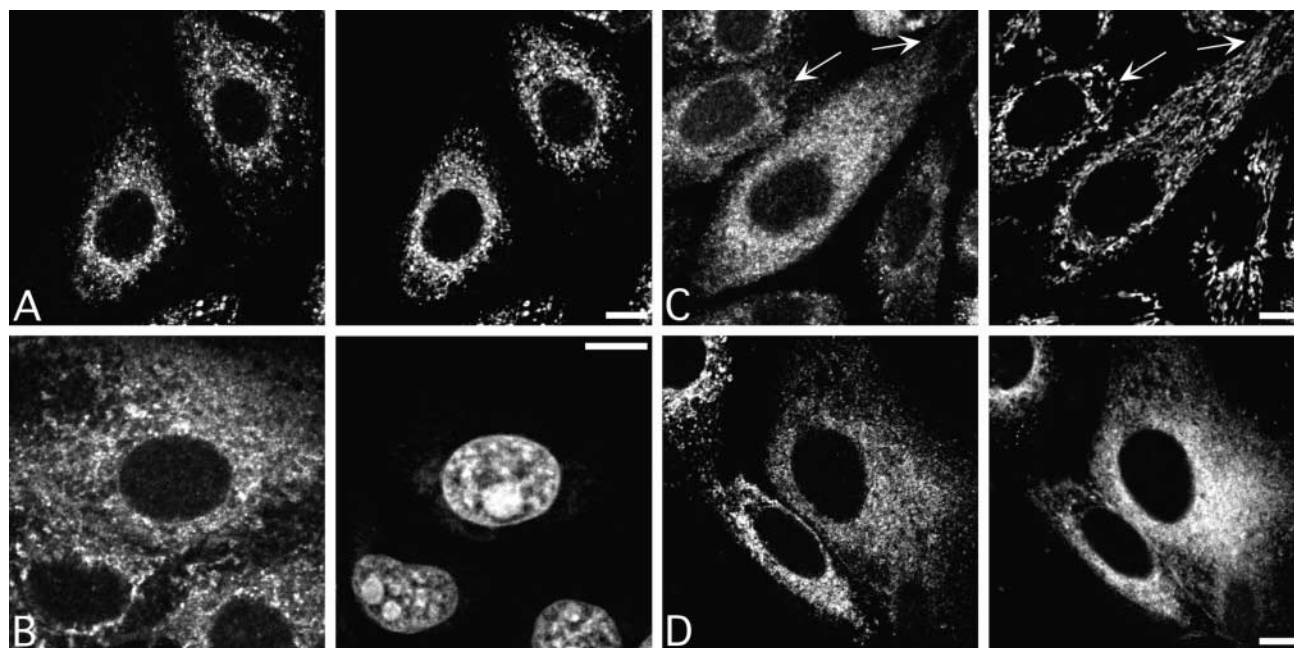


Figure 2 Comparative immunolocalization of ERp29 to the ER/nuclear envelope in MDCK cells. Canine kidney epithelial cells (MDCK) growing on glass coverslips were double-labeled with anti-ERp29 (left panels) and four comparative markers (right panels), then examined in parallel by confocal microscopy. (A) ERp29 exhibited a reticular perinuclear distribution equivalent to that of BiP, an archetypal marker of the ER lumen. (B) The perinuclear boundary of ERp29 staining coincided with the nuclear envelope delineated by propidium iodide, a DNA stain. (C) In contrast to the reticular and predominantly perinuclear labeling of ERp29, antibodies to mitochondrial cytochrome c oxidase revealed rod-shaped mitochondria evenly distributed throughout the cells. Arrows indicate ERp29-poor regions that contain mitochondria. (D) Concanavalin A, a marker of the ER membrane, had the same topographical distribution as ERp29. Although reticular, the concanavalin A pattern was more uniform than the soluble ER residents (ERp29, BiP). Weak intranuclear labeling was evident in some preparations, both with anti-ERp29 (e.g., B,C) and in nonimmune controls (not shown), and so was considered nonspecific (Melan and Sluder 1992). All other immunolabeling referred to in this figure and elsewhere was specific, as judged by comparison with controls (not shown). Bars = 5 μ m.

Rat liver microsomes were subfractionated using a classical sucrose density gradient procedure and analyzed by quantitative immunoblotting (Figure 3). When equal protein loads were compared, ERp29 was detected most strongly in the rough microsomes but substantial amounts were also found to partition with the less-dense fractions that contain smooth ER and more distal elements of the secretory pathway. Densitometric analysis revealed a 2.4 ± 0.2 -fold difference (\pm SEM; $n = 5$ from two preparations) in ERp29 content between the least- and most-enriched fractions. A similar enrichment was observed for BiP, whereas PDI was more evenly distributed across the gradient (Figure 3), consistent with previous reports (Ohba et al. 1981; Villa et al. 1992). This result suggested that ERp29 was predominantly associated with, but not restricted to, the rough ER of rat liver.

ERp29 Is Expressed in Diverse Cell Types

We undertook an extensive immunohistochemical analysis to establish whether the broad tissue distribution (Hubbard et al. 2000) reflected ERp29 expression in diverse cell types as opposed to a few cell types that are broadly distributed (Table 1; Figure 4). ERp29 immunostaining was detected specifically in more than 35 functionally different cell types that represented all major classes of tissue (epithelia, neural, connective tissue, blood, muscle) in rat. The strongest ERp29 labeling was observed in secretory ameloblasts of the dental enamel organ, Type 2 alveolar cells in lung, Purkinje neurons in cerebellum, precursor lymphocytes in spleen (Figure 4), and alveolar cells of the lactating mammary gland. All these cell types are recognized to have heavy protein-secretory duties. In contrast, ERp29 labeling was weaker in cells that primarily se-

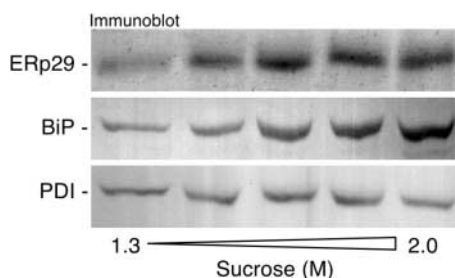


Figure 3 Predominant localization of ERp29 to rough microsomes on sucrose gradients. Rat liver microsomes were subfractionated by sedimentation through a discontinuous sucrose gradient, harvested from the 1.3–2 M sucrose region, and then subjected to parallel immunoblotting analysis with anti-ERp29, anti-BiP, and anti-PDI as indicated. Protein loads were equated on the basis of Coomassie-stained gels (not shown). ERp29 was detected most strongly in the denser fractions, similar to BiP, whereas PDI was more evenly distributed. All panels are sections of a single blot and show the regions corresponding to 29 kD (ERp29), 55 kD (PDI), and 78 kD (BiP). The immunodetection was specific (cf. Figure 1) and no other major bands were detected outside the regions shown.

crete lipids or carbohydrates (e.g., sebaceous adipocytes, salivary epithelial cells). A good correspondence existed between the ERp29 expression levels suggested by immunohistochemistry (Table 1) and the ranking determined previously at the tissue level by quantitative immunoblotting (Hubbard et al. 2000). In dental enamel epithelium, the most enriched tissue identified to date, ERp29 was strongly represented in the elongate ameloblasts that secrete enamel proteins but not in the overlying accessory cells (Figure 4A). Much lower levels of ERp29 were detected in the dentine-secreting cells (odontoblasts) and adjacent dental mesenchyme (pulp), whereas the extracellular matrices (enamel, dentine) were devoid of ERp29 immunoreactivity (Figure 4A), as anticipated from previous immunoblotting data (Hubbard et al. 2000). Although a minority of cells had immunostaining close to background and therefore of uncertain specificity (e.g., striated muscle fibers; Table 1), these results suggested that ERp29 might be expressed in essentially all types of cell.

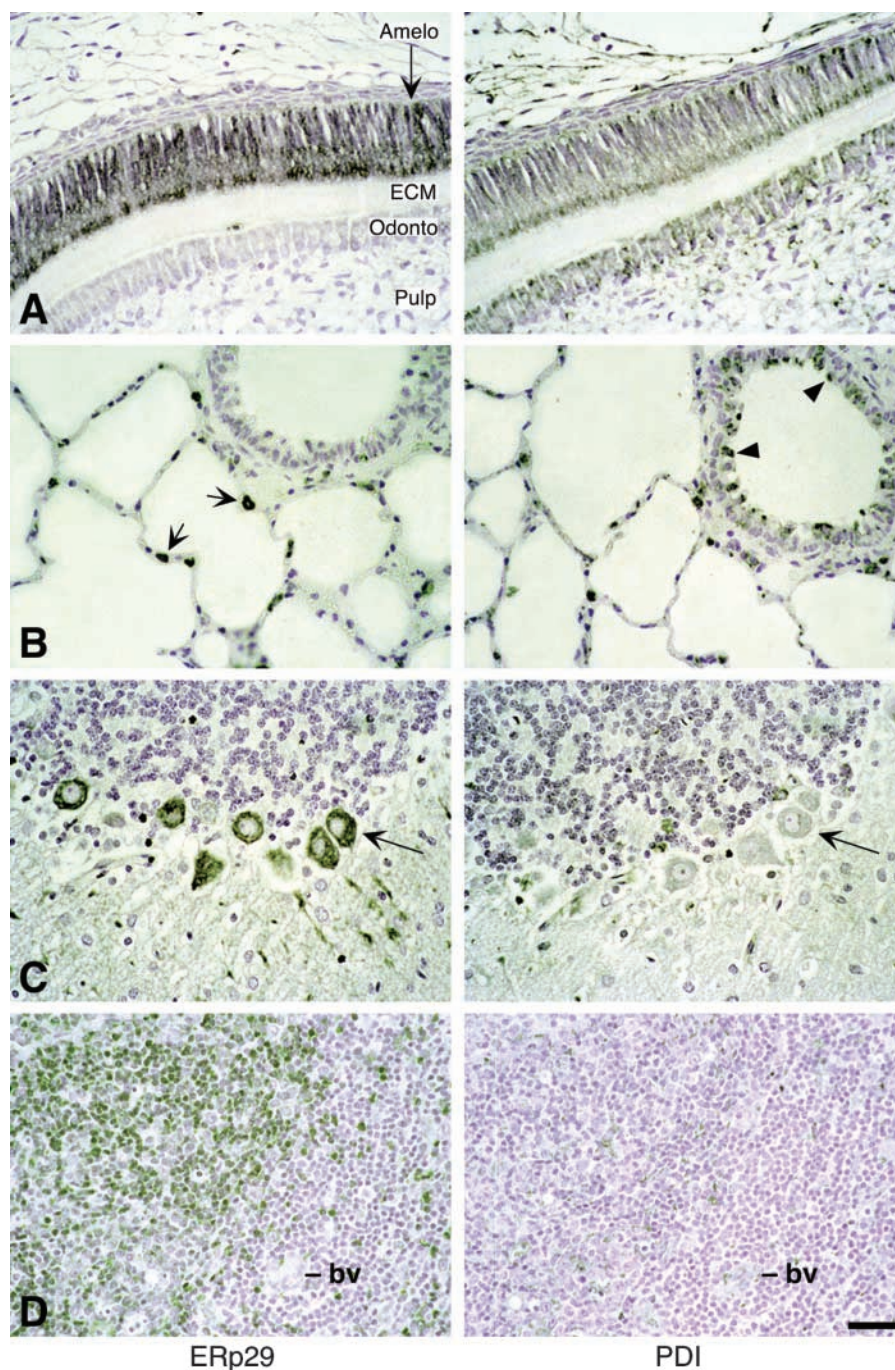
ERp29 and PDI Have Overlapping but Distinct Cellular Expression Patterns

We earlier postulated that ERp29 has a unique role in secretory protein synthesis, based on the novel sequence and varied tissue expression patterns relative to other reticuloplasmins (Demmer et al. 1997; Hubbard et al. 2000). To test this idea at the cellular level, we compared the distributions of ERp29 and PDI immunohistochemically. The observed PDI immunostaining patterns showed a general correspondence to the distribution of ERp29 (Table 1) and were consistent with previous reports (Kasper et al. 1994; Iida et al. 1996). However, several striking differences were observed (Figure 4). In the developing tooth, PDI staining was strong in ameloblasts and odontoblasts, unlike ERp29, which was abundant in ameloblasts only. In lung, the bronchiolar Clara cells were highly immunopositive for PDI but not for ERp29, whereas both proteins were detected strongly in type 2 alveolar cells. In cerebellum, Purkinje neurons were strongly labeled for ERp29 but not for PDI. In spleen, immature white cells were highly reactive for ERp29 but not for PDI. Less obvious differences were observed elsewhere. In pancreas, for example, ERp29 was detected more strongly in the endocrine islet cells than in the exocrine acini, whereas the reverse pattern was observed for PDI (Table 1). These findings suggested that the relative abundances of ERp29 and PDI vary markedly between some cell types, consistent with independent regulatory and functional roles.

Discussion

This study ratifies the broad biological relevance of ERp29 by revealing a ubiquitous cellular distribution

Figure 4 Comparative immunolocalization of ERp29 and PDI in rat tissues. Consecutive paraffin sections of various rat tissues were probed in parallel with anti-ERp29 and anti-PDI as indicated. ERp29/PDI immunolabeling is green-brown-black and unlabeled nuclei appear blue due to hematoxylin counterstaining. (A) Developing rat tooth (second mandibular molar from a 14-day-old pup), showing exceptionally strong ERp29 labeling of secretory ameloblasts (Amelo). ERp29 was detected more weakly in the stellate cells of the enamel organ (top of field), the pulp fibroblasts, and odontoblasts (Odonto), and was absent from enamel and dentinal extracellular matrices (ECM). In contrast, PDI was detected at moderate levels in all these cell types. (B) Lung, including alveolar sacs and a terminal bronchiole (top right of field). ERp29 labeling was strong in cuboidal Type 2 alveolar cells (arrows) and weak in other cells of the alveolus and bronchiole. PDI exhibited an equivalent pattern except that bronchiolar Clara cells were labeled strongly (arrowheads). The localization of ERp29 to Type 2 alveolar cells was confirmed with isolated cells (D. Warburton and MJH, unpublished results). (C) Cerebellum, with the large Purkinje cells (arrows) interposed between granule cell and molecular layers (upper and lower half of field, respectively). ERp29 was detected strongly in Purkinje cells but not elsewhere. In contrast, PDI labeling was weak in Purkinje cells and moderate in granule cells. (D) Spleen, showing white pulp largely populated by lymphocyte precursors undergoing development from larger immature forms (top left of field) to more mature cells (bottom right). ERp29 was detected more strongly in immature cells, unlike PDI, which exhibited relatively low and homogeneous labeling. The ERp29 and PDI fields were aligned with reference to blood vessels (bv). The green color balance was increased to enhance contrast between immunolabel and the dense nuclear background. All the noted differences between ERp29 and PDI (A–D) were verified in other experiments in which different antibody concentrations and development times were used. Bar = 50 μ m.



in rat. A principal localization to protein secretory cells and to rough ER supports the hypothesis that ERp29 functions primarily in the early stages of secretory protein production. The notion that ERp29 has a different role from that of its closest structural relative, PDI, is also supported by evidence of divergent cellular expression profiles in several tissues. Collectively, these results establish ERp29 as a general ER marker and suggest that it has a distinct role with potential selectivity for non-collagenous polypeptides.

The widespread cellular distribution established in this study indicates that ERp29 has a functional role of general utility rather than a specialist one used by a minority of cells. ERp29 can be considered ubiquitous because it has now been detected in over 30 different tissues from human and rat (Hubbard and McHugh 2000; Hubbard et al. 2000; and this study). However, it remains to be established whether ERp29 is expressed in all ER-containing cells. Previously, we found that the specific abundance of ERp29 varied over

quite a narrow range in most rat tissues (about four-fold vs >30-fold for BiP) (Hubbard et al. 2000). Concordantly, in this study muscle was one of only a few cell types found to have minimal ERp29 immunostaining (Table 1). The low ERp29 signal in muscle is consistent with low levels of transcript and protein observed previously by Northern and immunoblotting analyses (Demmer et al. 1997; Hubbard et al. 2000) and parallels the low abundance of other reticuloplasmins (Khanna and Waisman 1986; Iida et al. 1996). Our findings are likely to apply more broadly in the animal kingdom because we have recently confirmed the presence of ERp29 in chicken liver (Swiss Protein database, accession P81628). However, yeasts appear to lack ERp29 (like calreticulin, endoplasmic reticulum chaperone, ERp60, and ERp72) and to date there is no evidence of an ERp29 homologue in plants.

ERp29 can now be considered a general ER marker, given the evidence here of an exclusive ER location and ubiquitous cellular distribution. Comparison with a variety of ER markers (both luminal and membrane) consistently localized ERp29 to the ER/nuclear envelope and, together with sucrose gradient analysis (Figures 2 and 3), indicated that ERp29 resides throughout the rough/smooth-ER continuum like other major reticuloplasmins (Bole et al. 1989; Bergmann and Fusco 1990; Villa et al. 1993). Likewise, ERp29 appeared to be substantially excluded from the Golgi complex (Figure 2D), in agreement with earlier subcellular fractionation results (Ferrari et al. 1998). The lack of ERp29 immunolocalization to mitochondria and cytosol of fixed MDCK cells corroborates our earlier proteomic finding with semi-intact enamel cells (Hubbard et al. 2000). Consequently, it appears likely that the conflicting finding of ERp29 in a crude mitochondrial fraction of homogenized liver reflected incomplete resolution from nuclei and microsomes, both of which had much higher ERp29 contents (Hubbard et al. 2000). Although the immunolocalization and biochemical data are collectively consistent with ERp29 being located in the ER only, it would be premature to dismiss minor representations in other locations as appears likely for some reticuloplasmins (Takemoto et al. 1992; Michalak et al. 1999; Holaska et al. 2001).

Our results associate ERp29 with early production events of secretory proteins through a PDI-like cellular expression profile and a BiP-like predominance in rough ER. Conversely, dominant roles in lipogenesis, glycosylation, or calcium storage were opposed by the finding of ERp29 at generally lower levels in lipid- and carbohydrate-oriented cells (adipocytes, hepatocytes, salivary epithelium) and in smooth ER (Table 1; Figure 3). It is now apparent that ERp29 is one of the most abundant reticuloplasmins in a variety of cells, including ameloblasts, Type 2 alveolar cells, and Purkinje neurons, because near-equimolarity with PDI and BiP

was found at the corresponding tissue level (Hubbard et al. 2000). It follows that in such cells ERp29 will be sufficiently abundant to participate in stoichiometric interactions with principal secretory proteins, as is characteristic of chaperones and foldases. Preliminary evidence of interactions between ERp29 and proteins in the ER has been obtained using immunoprecipitation and crosslinking approaches (Ferrari et al. 1998; Mkrtchian et al. 1998a,b) but more detailed investigations are needed to clarify the functional significance.

Despite the general parallels with other protein-centric reticuloplasmins, our data support the notion that ERp29 is independently regulated and has a distinct role in secretory protein production, perhaps related to particular types of nascent polypeptide. The new finding that PDI and ERp29 have different cellular abundance profiles (Table 1; Figure 4) is consistent with non-equivalent functions as previously inferred from the primary structures and tissue expression levels (Demmer et al. 1997; Hubbard et al. 2000). We can now identify various cell types in which ERp29 is likely to play a major role (e.g., ameloblasts, Type 2 alveolar cells, Purkinje neurons) and other types of cell that, although secretory, appear to be less dependent on ERp29 (e.g., odontoblasts, Clara cells, cerebellar granule cells). Given this broad dependence on cell type, an ensuing question is whether ERp29 expression levels are linked to particular attributes of the secretory proteins produced. In the developing tooth, ameloblasts primarily secrete a hydrophobic non-collagenous protein (amelogenin) that differs markedly from the major product of odontoblasts, Type 1 collagen (Simmer and Fincham 1995). Importantly, the resultant extracellular matrices (i.e., pre-enamel and predentine) are produced in parallel, suggesting that abundant expression of ERp29 in ameloblasts does not simply reflect a higher secretory rate. In lung, Type 2 alveolar cells and Clara cells produce largely overlapping sets of secretory proteins. However, the ERp29-deficient Clara cells do not secrete a hydrophobic protein (surfactant protein C) that is a major product of Type 2 alveolar cells, and the alveolar cells do not secrete the hydrophilic Clara cell-specific protein that is unique to Clara cells (Khour et al. 1996; Zhou et al. 1996). Secretory products of Purkinje and granule cells are not well characterized to our knowledge but, as one of the largest and most heavily synapsed neurons in brain, Purkinje cells face significant demands for protein export to the plasma membrane (e.g., postsynaptic receptors). Neuromodulatory and trophic factors are also understood to be secreted by Purkinje cells (Strata and Rossi 1998; Sluck et al. 1999) but, intriguingly, protein-centric reticuloplasmins are expressed at relatively low levels in these cells despite a heavy enrichment with calcium-handling ER proteins (Villa et al. 1992; Nori et al. 1993; Hubbard

and McHugh 2000). Consequently, we predict that ERp29 expression is not crucial for the production of collagenous proteins (the low ERp29 level evident in odontoblasts also holds for chondrocytes and dermal fibroblasts; Table 1) but perhaps is beneficial for hydrophobic proteins such as amelogenins, surfactant proteins, and membrane receptors. Precedents exist for such selectivity among the major reticuloplasmic proteins, which are generally regarded as having broad substrate specificity. For example, PDI expression is linked most strongly to production of disulfide-bonded and collagenous proteins, yet other members of the PDI family show distinct cellular expression patterns consistent with different substrate preferences (Freedman 1984; Iida et al. 1996; Desilva et al. 1997; Ferrari and Soling 1999). Likewise, although BiP can interact with a broad variety of polypeptides, its highest-affinity interaction is with a particular subclass of nascent proteins defined by hydrophobicity and folding kinetics (Hellman et al. 1999; Knarr et al. 1999).

In conclusion, this study has produced novel cellular evidence that the role of ERp29 is of general utility, primarily involved in early phases of secretory protein production, and different from that of PDI. Having now established a fundamental understanding of ERp29 location and cellular expression patterns, it should be informative to reappraise functional properties of isolated ERp29, to refine the localization in ER subcompartments, and to characterize protein interactions with ERp29. Importantly, this study has identified a variety of physiologically relevant cellular settings in which to pursue such investigations.

Acknowledgments

Supported by NZ Lottery Health Research and the Health Research Council (NZ). MJH is a Senior Research Fellow of the NZ Health Research Council.

We thank Patricia Flawn and Nicky McHugh for skilled biochemical assistance, Jennifer Macleod for assisting with neonatal rat perfusions, Ken Turner for histological advice, and our other colleagues who provided constructive comments and support.

Literature Cited

- Argon Y, Simen BB (1999) GRP94, an ER chaperone with protein and peptide binding properties. *Semin Cell Dev Biol* 10:495–505
- Bergmann JE, Fusco PJ (1990) The G protein of vesicular stomatitis virus has free access into and egress from the smooth endoplasmic reticulum of UT-1 cells. *J Cell Biol* 110:625–635
- Bole DG, Dowin R, Doriaux M, Jamieson JD (1989) Immunocytochemical localization of BiP to the rough endoplasmic reticulum. Evidence for protein sorting by selective retention. *J Histochem Cytochem* 37:1817–1823
- Corbett EF, Michalak M (2000) Calcium, a signaling molecule in the endoplasmic reticulum? *Trends Biochem Sci* 25:307–311
- Demmer J, Zhou CM, Hubbard MJ (1997) Molecular cloning of ERp29, a novel and widely expressed resident of the endoplasmic reticulum. *FEBS Lett* 402:145–150
- Desilva MG, Notkins AL, Lan MS (1997) Molecular characterization of a pancreas-specific protein disulfide isomerase, PDIp. *DNA Cell Biol* 16:269–274
- Ellgaard L, Molinari M, Helenius A (1999) Setting the standards. Quality control in the secretory pathway. *Science* 286:1882–1888
- Ferrari DM, Nguyen Van P, Kratzin H, Soling HD (1998) ERp28, a human endoplasmic reticulum luminal protein, is a member of the protein disulfide isomerase family but lacks a CXXC thioredoxin-box motif. *Eur J Biochem* 255:570–579
- Ferrari DM, Soling HD (1999) The protein disulphide-isomerase family: unravelling a string of folds. *Biochem J* 339:1–10
- Freedman RB (1984) Native disulphide bond formation in protein biosynthesis. Evidence for the role of protein disulphide isomerase. *Trends Biochem Sci* 9:438–441
- Gething MJ (1999) Role and regulation of the ER chaperone BiP. *Semin Cell Dev Biol* 10:465–472
- Gething MJ, Sambrook J (1992) Protein folding in the cell. *Nature* 355:33–45
- Hellman R, Vanhove M, Lejeune A, Stevens FJ, Hendershot LM (1999) The in vivo association of BiP with newly synthesized proteins is dependent on the rate and stability of folding and not simply on the presence of sequences that can bind to BiP. *J Cell Biol* 144:21–30
- Holaska JM, Black BE, Love DC, Hanover JA, Leszyk J, Paschal BM (2001) Calreticulin is a receptor for nuclear export. *J Cell Biol* 152:127–140
- Honore B, Vorum H (2000) The CREC family, a novel family of multiple ER-hand, low affinity Ca²⁺-binding proteins localised to the secretory pathway of mammalian cells. *FEBS Lett* 466:11–18
- Hortsch M, Meyer DI (1985) Immunochemical analysis of rough and smooth microsomes from rat liver. Segregation of docking protein in rough microsomes. *Eur J Biochem* 150:559–564
- Hubbard MJ (1995) Calbindin_{28kDa} and calmodulin are hyperabundant in rat dental enamel cells: identification of the protein phosphatase calcineurin as a principal calmodulin target and of a secretion-related role for calbindin_{28kDa}. *Eur J Biochem* 230:68–79
- Hubbard MJ, McHugh NJ (2000) Human ERp29: isolation, primary structural characterisation and two-dimensional gel mapping. *Electrophoresis* 21:3785–3796
- Hubbard MJ, McHugh NJ, Carne DL (2000) Isolation of ERp29, a novel endoplasmic reticulum protein, from rat enamel cells: evidence for a unique role in secretory-protein synthesis. *Eur J Biochem* 267:1945–1956
- Iida KI, Miyaiishi O, Iwata Y, Kozaki KI, Matsuyama M, Saga S (1996) Distinct distribution of protein disulfide isomerase family proteins in rat tissues. *J Histochem Cytochem* 44:751–759
- Kasper M, Fuller SD, Schuh D, Muller M (1994) Immunohistochemical detection of the b subunit of prolyl 4-hydroxylase in rat and mini pig lungs with radiation-induced pulmonary fibrosis. *Virchows Arch* 425:513–519
- Khanna NC, Waisman DM (1986) Development of a radioimmunoassay for quantitation of calregulin in bovine tissues. *Biochemistry* 25:1078–1082
- Khoor A, Gray ME, Singh G, Stahlman MT (1996) Ontogeny of Clara cell-specific protein and its mRNA. Their association with neuroepithelial bodies in human fetal lung and in bronchopulmonary dysplasia. *J Histochem Cytochem* 44:1429–1438
- Knarr G, Modrow S, Todd S, Gething MJ, Buchner J (1999) BiP-binding sequences in HIV gp160. Implications for the binding specificity of BiP. *J Biol Chem* 274:29850–29857
- Kreibich G, Ulrich BL, Sabatini DD (1978) Proteins of rough microsomal membranes related to ribosome binding. I. Identification of ribophorins I and II, membrane proteins characteristic of rough microsomes. *J Cell Biol* 77:464–487
- Liepinsh E, Baryshev M, Shapiro A, Ingelman-Sundberg M, Otting G, Mkrtchian S (2001) Thioredoxin fold as homodimerization module in the putative chaperone ERp29. NMR structures of the domains and experimental model of the 51kDa dimer. *Structure* 9:457–471
- Meier KE, Snaveley MD, Brown SL, Brown JH, Insel PA (1983) α_1 -

- and β_2 -adrenergic receptor expression in the Madin-Darby canine kidney epithelial cell line. *J Cell Biol* 97:405–415
- Melan MA, Sluder G (1992) Redistribution and differential extraction of soluble proteins in permeabilised cultured cells. Implications for immunofluorescence microscopy. *J Cell Sci* 101: 731–743
- Mentlein R, Rix-Matzen H, Heymann E (1988) Subcellular localization of non-specific carboxylesterases, acylcarnitine hydrolase, monoacylglycerol lipase and palmitoyl-CoA hydrolase in rat liver. *Biochim Biophys Acta* 964:319–328
- Michalak M, Corbett EF, Mesaeli N, Nakamura K, Opas M (1999) Calreticulin. One protein, one gene, many functions. *Biochem J* 344:281–292
- Mkrtchian S, Baryshev M, Matvijenko O, Sharipo A, Sandalova T, Schneider G, Ingelman-Sundberg M (1998a) Oligomerization properties of ERp29, an endoplasmic reticulum stress protein. *FEBS Lett* 431:322–326
- Mkrtchian S, Fang C, Hellman U, Ingelman-Sundberg M (1998b) A stress-inducible rat liver endoplasmic reticulum protein, ERp29. *Eur J Biochem* 251:304–313
- Nori A, Villa A, Podini P, Witcher DR, Volpe P (1993) Intracellular Ca^{2+} stores of rat cerebellum. Heterogeneity within and distinction from endoplasmic reticulum. *Biochem J* 291:199–204
- Ohba H, Harano T, Omura T (1981) Intracellular and intramembranous localization of a protein disulfide isomerase in rat liver. *J Biochem* 89:889–900
- Parodi AJ (2000) Protein glycosylation and its role in protein folding. *Annu Rev Biochem* 69:69–93
- Pozzan T, Rizzuto R, Volpe P, Meldolesi J (1994) Molecular and cellular physiology of intracellular calcium stores. *Physiol Rev* 74: 595–636
- Satoh T, Hosokawa M (1998) The mammalian carboxylesterases. From molecules to functions. *Annu Rev Pharmacol Toxicol* 38: 257–288
- Simmer JP, Fincham AG (1995) Molecular mechanisms of dental enamel formation. *Crit Rev Oral Biol Med* 6:84–108
- Sluck JM, Lin RC, Katolik LI, Jeng AY, Lehmann JC (1999) Endothelin converting enzyme-1-, endothelin-1-, and endothelin-3-like immunoreactivity in the rat brain. *Neuroscience* 91:1483–1497
- Strata P, Rossi F (1998) Plasticity of the olivocerebellar pathway. *Trends Neurosci* 21:407–413
- Takemoto H, Yoshimori T, Yamamoto A, Miyata Y, Yahara I, Inoue K, Tashiro Y (1992) Heavy chain binding protein (BiP/GRP78) and endoplasmin are exported from the endoplasmic reticulum in rat endocrine pancreatic cells, similar to protein disulfide-isomerase. *Arch Biochem Biophys* 296:129–136
- Urban J, Parczyk K, Leutz A, Kayne M, Kondor-Koch C (1987) Constitutive apical secretion of an 80-kD sulfated glycoprotein complex in the polarized epithelial Madin-Darby canine kidney cell line. *J Cell Biol* 105:2735–2743
- Villa A, Podini P, Panzeri MC, Soling HD, Volpe P, Meldolesi J (1993) The endoplasmic-sarcoplasmic reticulum of smooth muscle. Immunocytochemistry of vas deferens fibers reveals specialized subcompartments differently equipped for the control of Ca^{2+} homeostasis. *J Cell Biol* 121:1041–1051
- Villa A, Sharp AH, Racchetti G, Podini P, Bole DG, Dunn WA, Pozzan T, Snyder SH, Meldolesi J (1992) The endoplasmic reticulum of Purkinje neuron body and dendrites. Molecular identity and specializations for Ca^{2+} transport. *Neuroscience* 49:467–477
- Wood JG, McLaughlin BJ, Barber RP (1974) The visualisation of concanavalin A binding sites in Purkinje cell somata and dendrites of rat cerebellum. *J Cell Biol* 63:541–549
- Zhou L, Lim L, Costa RH, Whitsett JA (1996) Thyroid transcription factor-1, hepatocyte nuclear factor-3 β , surfactant protein B, C, and Clara cell secretory protein in developing mouse lung. *J Histochem Cytochem* 44:1183–1193